ChemPubSoc Europe

DOI: 10.1002/open.201800121

Open Access ChemistryOPEN Full Papers

Specific Residue Interactions Regulate the Binding of Dengue Antigens to Broadly Neutralizing EDE Antibodies

Mauro Lapelosa,*[a] Oscar Burrone,[b] and Walter Rocchia*[a]

Antibodies binding to antigens present on the dengue virus (DENV) represent the main defense mechanism of the host organism against the pathogen. Among the antibodies elicited by DENV and that bind to DII of protein E, EDE1-C8 can bind all DENV serotypes. Our analysis reveals the key residues in this interaction as well as structurally conserved hydrogen bonds located at the binding interface. They stabilize the dengue antigen–antibody complex among the EDE1 group of antibodies (Abs). Combining structural alignments with molecular dynamics simulations in the EDE1 Abs, we identified the critical elements that provide a major energetic contribution to the association of antigens from protein E with Abs. We discuss possible molecular insights into the binding mechanism by using a surrogate molecular entity resembling the protein E that forms native salt bridges and hydrogen bonds, including inferences on the light of high-resolution crystal structures of dengue Fab complexes. Finally, the molecular determinants, the free energy profile, and the binding mechanism provide inspiration for potential strategies in protein engineering to design novel immunogens of protein E against DENV.

1. Introduction

Epidemics from infectious viral diseases pose a global threat to human health. Infection with the dengue virus (DENV) affects 400 million people globally, constituting a major health issue, particularly for the 100 million people that manifest severe symptoms (dengue hemorrhagic fever). There is great interest from both academic and industrial researchers to conduct studies on structure and function analysis, infection source and route, therapeutic targets, vaccines, and therapeutic drugs.[1] The targets against DENV include NS3/NS2B protease, NS3 helicase, envelope (E) protein, methyltransferase (MTase), RNA-dependent RNA polymerase of NS5, and the host factors in the lifecycle of the virus. Protein E is a 53 kD protein composed of three domains and exposed on the surface of the virions. In the virus cycle, protein E plays a major role in virus entry into the host cells. Furthermore, it represents a central protein in dengue, because it is the only protein targeted by neutralizing antibodies that are capable of blocking virus entry into the host cells. The design of novel immunogens containing potent molecular determinants and capable of triggering a neutralizing immune response represents a central strategy to fight against DENV, and computer-aided approaches can speed up this process.[2]

Most residues of protein E have been solved with X-ray crystallography and assume a conformational arrangement similar to the one in the virion particles.[3] A series of broadly neutralizing antibodies have been isolated from infected patients, and the crystal structures of the complexes with protein E in the dimer form have been solved at 3 Å resolution.[4] They can be classified into two groups according to their ability to bind the target in the presence of glycosylation or not. EDE1 represents the first group, which does not require glycosylation to bind efficiently, and it includes the antibodies C8 and C10. Conversely, EDE2 includes A11 and B7. In the search for key residues contributing to the interaction across the different antibodies, we have performed structural alignment of four antibodies: C8, C10, A11, and B7. Protein E interacts in a similar way with all of them, and the residues on protein E interacting at the binding interface are conserved among the four serotypes, explaining the reason behind their cross-reactivity. Interestingly, we can identify a set of amino acids that constitute major molecular determinants in the formation of the antigen–antibody complex analyzed by superimposing the crystal structure of the EDE Abs complexes. After this analysis, we designed a surrogate structural model derived from protein E that allowed us to run molecular dynamics simulations and free energy calculations, otherwise prohibitive due to the large size of the system. This novel design can represent an antigen analogue for DENV. Molecular dynamics simulations provided information about the fluctuations within the antigen–Fab complex, and allowed us to obtain a per-residue energy decomposition of the interacting residues. The free energy change from the bound to unbound state of about 5 kcal mol^{-1}, which supports a favorable binding interaction between

[a] Dr. M. Lapelosa, Dr. W. Rocchia
CONCEPT Lab
Department of Drug Discovery and Development
Italian Institute of Technology
Genova, viaMorego 60, 16163 (Italy)
E-mail: maurolap@gmail.com
walter.rocchia@iit.it

[b] Dr. O. Burrone
Department of Molecular Immunology
ICGEB-International Center for Genetic Engineering and Biotechnology
Trieste, Via Padriciano 99, 34149 (Italy)

Supporting Information and the ORCID identification number(s) for the author(s) of this article can be found under: https://doi.org/10.1002/open.201800121.

the considered molecules, was calculated from the potential of mean force (PMF). The simulated binding trajectory allowed us to detect a structural intermediate, pointing to key molecular elements for ensuring ligand specificity and binding efficiency. This novel intermediate can also disclose molecular details about key contacts that are important in the development of novel antigen-mimicking protein E. A key hydrogen bond between Gly 104 and Asn 93 in the light chain, a salt bridge between Lys 247 and Asp 56 in the heavy chain, and a hydrophobic contact between Trp 101 and Phe 32 in the light chain anchor the antigen to the Fab receptor. These structural determinants constitute the driving force for potency and specificity of the antigen to the EDE, broadly neutralizing Abs.

Computational Methods

Molecular Dynamics (MD) Simulations

The structure of EDE1 C8 Fab bound to protein E was retrieved from the protein data bank (PDB ID: 4UTA).[4,5] The initial structure of the surrogate protein was obtained including the b strand, the fusion loop and the ij loop. The new protein consisted of 83 residues and the "150 loop" region was eliminated. This model was obtained with MODELLER software,[6,7] using the structure of 4UTA as a template. This template was selected over the other EDE Fab–antigen crystal structures because, in this complex, the antigen–antibody forms the largest number of contacts. A MD run on the selected model after the homology modeling was performed. The crystallographic water molecules were eliminated. Ionization states were assigned considering neutral pH, and hydrogen atoms were added by using the Psfgen utility in VMD. A box with explicit water molecules was built to solvate the protein. The final system consisted of a total of 17374 atoms, including the water molecules and ions to neutralize the net charge of the system. The energy minimization was carried out for 5000 iterations and MD simulations were performed using NAMD v. 2.11[8] with the CHARMM36 force field[9] and TIP3P water model[10] with GPU acceleration.

Long-range electrostatics were computed by using particle-mesh Ewald (PME) summation.[11] The grid spacing was 1 Å. Van der Waals interactions were cut off beyond a distance of 9 Å by using a smooth function and covalent bonds involving hydrogens were kept fixed by using the SHAKE algorithm.[12] A Langevin thermostat was applied to control the temperature at 300 K, and the integration time step was 2 fs. The equilibration phase was 200 ps long at constant pressure ($P = 1.00$ bar) and temperature ($T = 300$ K) by using a Langevin Nosé–Hoover piston. Periodic boundary condition in Cartesian space were employed.

After this equilibration, the molecular dynamics run in the NVT ensemble were performed for 500 ns. The equilibrated structure from the MD trajectory was used for molecular docking onto the Fab EDE1 C8 receptor. The direct structural superimposition of the model on protein E in the crystal structure conformation would lead to atomic clashes, so protein docking was carried out. Docking was performed using ZDOCK software,[13,14] which uses a grid-based representation of the two proteins and a 6D fast Fourier transform (FFT) to efficiently perform the conformational search. Version 3.0.2 of ZDOCK[15] has a scoring function that includes shape complementarity, electrostatic forces, and a statistical potential for pairwise interactions.

Once the top pose of the complex was selected, a new set of MD simulations solvated with an explicit water model were performed. The total size of the system including the antigen and the Fab was 71311 atoms. The equilibration was performed as mentioned above for the single protein system. After the equilibration stage, the run was performed for 1 μs in the NVT ensemble. The adaptive biasing force (ABF) calculation[16,17] was carried out along the collective variable (CV), r, consisting in the distance separating the centers of mass between the receptor and the protein ligand, and an angular restraint was also applied. A flat-bottomed harmonic restraint was implemented to limit the angular motion of the ligand relative to the receptor. The angle θ, defined by one atom of the ligand (CA, Gly 44) and two atoms of the receptor (CA, Ile 51 of chain I and CA, Gln 90 of chain M), was restricted to have an oscillation of 70 degrees by using a harmonic potential with an upper and lower wall. A bias is applied, opposing the average force from the simulations to help the system cross barriers along the CV. The MD trajectory is going from the bound state ($r = 43.0$ Å) to the unbound state ($r = 58.0$ Å), avoiding the steric overlap in the bound state.[18] The ABF simulation was carried out for 500 ns. The PMF was obtained from the instantaneous force, which was collected in bins of 0.1 Å, integrating over the gradients obtained in the biased simulation. A total of 1500 samples of the force were collected before applying the bias onto r. The graphical representations of the proteins were produced by using CHIMERA[19] and VMD.[20] The ABF simulations used the CHARMM36 force field[9] and TIP3P water model[10] within the NAMD v. 2.11 molecular simulation package with GPU acceleration.[8] We used an automated approach to perform clustering analysis through the Ensemble Clustering approach.[21] This method is based on the average linkage definition and a penalty function to find a trade-off between the number of clusters and the spread in each cluster.

2. Results

2.1. Arg 99, Gly 104, and Lys 247 in Protein E Form the Main Interactions with EDE1 Abs

Structural alignment of EDE1 C8 and C10 Fabs at the interface region was used to identify the key residues providing enthalpic contributions to the antigen–EDE Abs binding (Figure 1). In EDE1 C8, Lys 247 of chain A from protein E forms a salt bridge with Asp 56 of the heavy chain of the Fab. A hydrogen bond between Gly 104 and Asn 93 of the light chain of the Fab anchors the antigen. Another hydrogen bond forms between the Arg 99 of the antigen and Asn 93. A hydrophobic contact occurs between Trp 101 of chain A and Phe 32 of the light chain. In EDE1 C10, the first salt bridge between Lys 247 and Asp 100 is conserved as in the EDE1 C8. One hydrogen bond between Gly 104 of the antigen and Asn 31 of the light chain is also present. Arg 99 forms hydrophobic contacts with Phe 103 of the heavy chain. Trp 101 of protein E is not interacting with Fab in this case. Overall, in the case of EDE1 C8, the total number of van der Waals contacts is about 103 against 67 contacts present in EDE1 C10. The interactions of residues Lys 247, Arg 99, and Gly 104 are also conserved in EDE2 A11 and B7. Lys 247 in the B7 forms contacts with its side chain instead of forming a salt bridge with an Asp in the Fab.

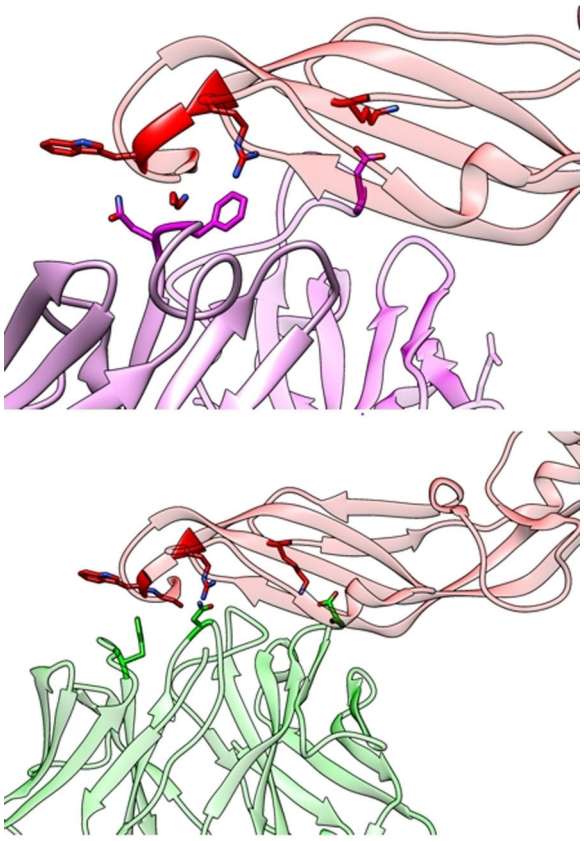

Figure 1. Structural alignment of conserved residues in the binding site for EDE1 C10 (top) and EDE1 C8 (bottom). The protein E residues are in red, EDE1 C10 Fab is in purple, and EDE1 C8 is in green.

2.2. Surrogate Antigen Model Docked onto EDE1 C8 Fab

An antigen model containing 83 residues from protein E was created to understand the dynamics of binding between antigen and EDE Abs. This model included key regions of protein E that associate with EDE Abs. The regions included in the surrogate model are the b strand, the fusion loop, and the ij loop. As these regions are not contiguous in the primary sequence of the original protein E, they were connected by using a loop of four residues (AAAG) (Figure 2). The top surrogate model, built as mentioned above, was used in the protein–protein docking. The best ranking pose docked on the EDE1 C8 Fab region showed a similar orientation to the parent protein E in the complex after superimposition, showing a RMSD of 0.45 Å between 62 pruned atoms. This pose was selected as the starting structure in the MD simulations, because of its structural similarity to the native protein E antigen structure.

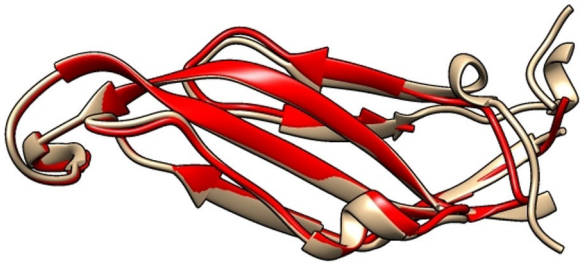

Figure 2. Top model of the surrogate structure (ribbon representation, in red) of the protein E antigen including b strand, the fusion loop, and the ij loop. The crystal structure of protein E is in sandy brown.

2.3. Antigen in the Complex Showed the Presence of Native Contacts Function Calculation

We used MD to further investigate the dynamics of the structural determinants in the antigen–EDE antibody binding. The conformation of the complex antigen–EDE1 C8 Fab retrieved by using docking was used in MD with an explicit solvent model. The complex had an equilibration stage from the initial structure in terms of backbone RMSD, but it stayed bound up to 1 μs replicated simulation. The distance between the centers of mass of the antigen and the EDE1 C8 Fab from the simulations fluctuates around the value (43 Å) of the bound pose (Figure 3). The center of mass (COM) distances of key hotspot amino acids are also at close range (Figure 4). Histograms of COM distances between Gly 104 and Asn 93, Lys 247 and Asp 56, and Trp 101 and Phe 32 present the most populated bins at similar values to those shown in the crystal structure. The value of COM residue distance in the crystal conformation (4UTA) is about 5.1 Å for Gly 104–Asn 93, 7.73 Å for Lys 247–Asp 56, and 8.36 Å for Trp 101–Phe 32. Per-residue energy decomposition of the residue at the interface provides the energetic contribution to the binding (Table 1). This analysis along the trajectory confirms the role of Gly 104, Lys 247 in the interaction, making it stable and emerging as hotspots in the antigen–EDE antibody association. Analyzing the hydrogen bonds formed by the antigen and the Fab receptor, we can find that, overall, the average number of hydrogen bond is 2.3, considering the entire structural ensemble. The main hydrogen bonds that hold the complex in the bound state involve Gly 104, Arg 99, and Lys 247, which, in addition to a salt bridge, can also form a hydrogen bond as a donor (Figure 5). These three hydrogen bonds are critical for the formation of the complex, and provide an enthalpic contribution that stabilizes the com-

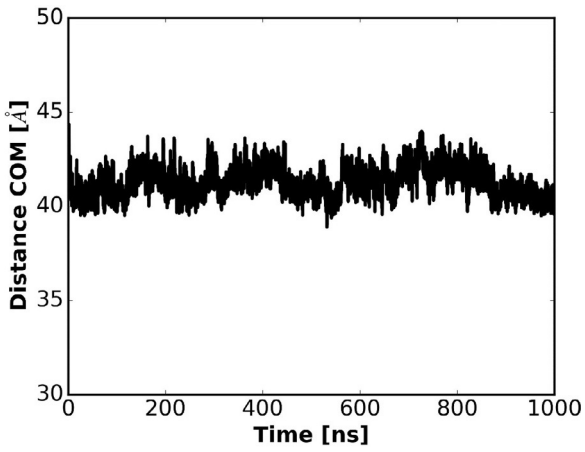

Figure 3. Time evolution of distance of COM between the antigen protein and the protein receptor in the unbiased MD simulation of 1 μs. The bound state is about 43 Å of COM distance.

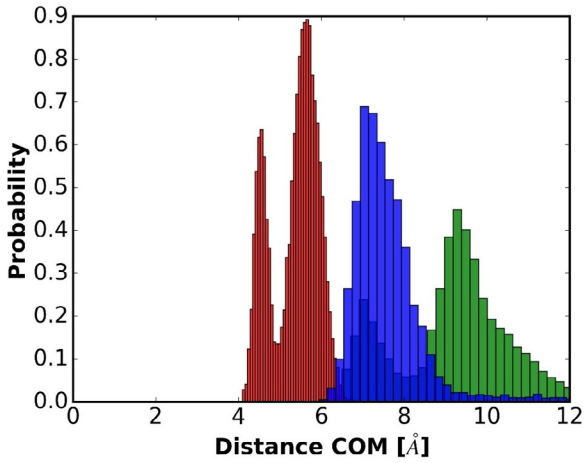

Figure 4. Histograms of COM distances for three conserved interactions obtained from the unbiased MD simulation of the antigen–Fab complex. In red, the histogram of the distances between Gly 104 of the antigen, and Asn 93 of the light chain of the Fab. In blue, the histogram of distances between Lys 247 of the antigen and Asp 56 of the heavy chain. In green, the histogram of distances between Trp 101 of the antigen and Phe 32 of the light chain. The value of COM–COM residue distance in the crystal conformation (4UTA) is about 5.1 Å for Gly 104–Asn 93, 7.73 Å for Lys 247–Asp 56, and 8.36 Å for Trp 101–Phe 32.

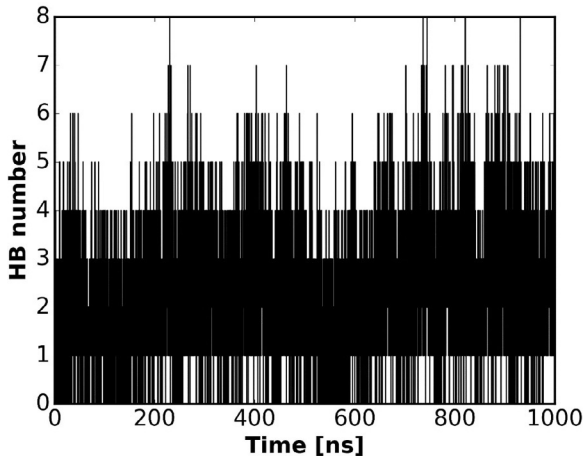

Figure 5. Number of intermolecular hydrogen bonds between the antigen and the EDE1 C8 Fab along the unbiased MD simulation.

Table 1. Per-residue energy decomposition of the antigen from protein E in the interaction with the Fab of EDE1 C8. The energies are calculated with the pair-wise additive function analysing the residue of the antigen at the interface from the unbiased molecular dynamics trajectory of the complex. The length of the trajectory was 1 μs.

Residue number	Average interaction energy [kcal mol^{-1}]	Standard deviation
Thr 68	−4.95	5.19
Thr 69	−2.00	3.12
Thr 70	−6.46	5.66
Glu 71	−13.56	14.45
Ser 72	−3.68	14.42
Trp 101	−2.68	3.50
Gly 102	−2.60	2.29
Asn 103	−5.73	5.03
Gly 104	−7.72	6.69
Cys 105	−2.62	2.73
Lys 246	−3.40	4.36
Lys 247	−93.51	75.74
Val 250	0.33	0.47

plex. Binding of a ligand on antigen and receptor protein changes the flexibility of certain parts of the protein, and affects its function. These changes are not uniform; some parts become more flexible and others become stiffer (Figure 6). Indeed, the antigen in the unbound state presents a large LGR-sheet region with high stability and flexible loops. Once the antigen binds to the EDE Fab part of the LGR-sheet region, it becomes flexible and the interface region becomes structurally stable. On the other hand, the flexible CDR loops of the Fab also increase their structural stability at the interface. The interior region of the fragment variable (Fv) part of Fab is stable in the bound state, whereas the exterior regions of the fragment crystallizable (Fc) part are more flexible.

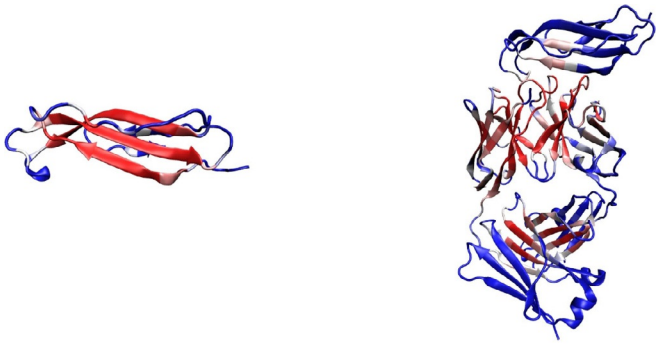

Figure 6. Time-averaged structure of the antigen surrogate model by itself (left) and in complex with EDE1 C8 Fab (right). It is calculated from two separate unbiased molecular dynamics runs one with the protein alone and the other with the protein in complex with the Fab. It is colored according to the B-factor calculated from the MD trajectories. Blue is greater than 50 Å^2, whereas red is less than 20 Å^2.

Evidence that the antigen stays bound in a long MD run with its core residues interacting with Fab provides a general indication of its capability to bind. Assuming an association rate constant (k_{on}) of 10^6 M^{-1} s^{-1} for the antigen and an equilibrium dissociation constant (K_d) in the millimolar range, the residence time should be greater than hundreds of microseconds. This makes the calculation of thermodynamic quantities from unbiased MD runs quite challenging, owing to the poor statistics that can be collected. Enhanced simulations methods[16,17,22–34] are needed to calculate the free energy for the antigen–EDE antibody association.

2.4. Free Energy Calculation

The free energy calculations were carried out by using the ABF method,[16,17,35] accelerating the sampling along the center-of-mass (COM) distance between the Fab receptor and the antigen protein. The Fab protein is the EDE1 C8, comprising a Ig fold characterized by a β-barrel topology. Our previous analysis has shown that this antigen assumes a stable conformation in the complex. The enhanced sampling was successful in detect-

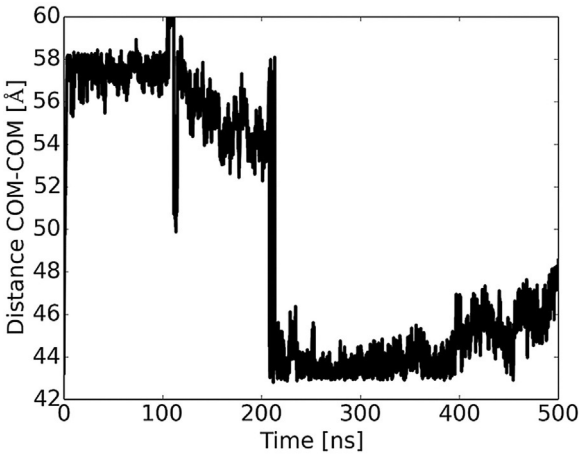

Figure 7. Time evolution of the distance of COM between the antigen binder and the Fab receptor in the ABF simulation with respect to the initial conformation of the complex.

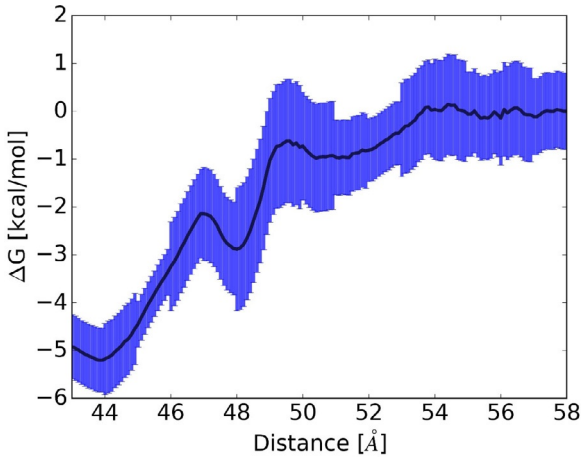

Figure 8. PMF profile for the reversible association of the antigen structure model with EDE1 C8 Fab calculated from the ABF simulation.

ing that the free energy has a minimum in the structure of the complex, and provided a free energy profile in the collective variable space. The dynamics observed in the ABF simulations shows how the peptide, starting from the bound conformation (Figure 7), stays bound for 5 ns (time is used as a measure of the simulation's progression, but loses its physical meaning due to the bias applied during the ABF simulation), then it dissociates from the receptor and reaches a distance value of 58 Å. At this point, the COM value oscillates around a value of about 57 Å, before decreasing to a value of 50 Å. At 200 ns, a binding event occurs, and the value decreases to 43 Å. After that, the antigen stays bound until 220 ns, and then it partially dissociates. At this point, it stays bound up to 400 ns, and then it moves again to the fully bound state at 450 ns.

The PMF contains useful thermodynamic information regarding the antigen–receptor binding process. In particular, the integration of the PMF yields the free energy of binding. The standard binding free energy (ΔG_b°), calculated from the PMF curve is about 5 kcal mol^{-1} $\pm$1.2, which is in agreement with the antigen binding. This value is expected to be different from that of the full protein E binding affinity, as we have replaced the full protein E with our surrogate antigen. The PMF (Figure 8) exhibits a deep minimum of approximately -5 kcal mol^{1} centered at 44.0 Å COM distance. Immediately beyond this distance, the PMF profile presents a peak corresponding to a partially bound state. Beyond 48.0 Å, the PMF increases rapidly to reach a distance of 50.0 Å at a value around -1. After this distance, the PMF increases very gradually, reaching an almost constant value at around 54.0 Å. The main free energy change to reach the unbound state occurs between 44.0 to 54.0 Å, where the PMF presents two steep slopes.

The clustering analysis was used to analyze the structural ensemble obtained in the ABF simulations. We could detect an intermediate structure in the unbinding process (Figure 9). This representative structure was obtained from the centroid of cluster 2, which includes a population of 8.2 (Table 2). This structure shows the antigen that hooks the Fab, forming an initial interaction between Gly 104 and Asn 93 of the Fab light

Figure 9. Intermediate structure along the binding trajectory found using the Ensemble clustering method forms contacts with Fab receptor. The antigen is highlighted in red, and is partially bound to the CDR region of the Fab (in green), forming transient interactions of Gly 104 with Asn 93 of the light chain.

Table 2. Top 15 clusters from the ABF simulation ensemble of 500 ns using the Ensemble clustering method. The total number of structures was 5301 with a step size of 1.

Cluster number	Population [%]	Representative frame
1	15.3	660
2	8.2	3680
3	6.7	4048
4	6.5	4669
5	6.3	1866
6	5.5	3394
7	5.3	932
8	5.1	3072
9	4.6	4271
10	4.5	1545
11	4.3	3870
12	4.2	5723
13	4.2	2248
14	3.9	3242
15	3.6	1140

chain. The formation of this interaction represents a key step in the mechanism of binding, because once this interaction is formed the antigen completely associates to the EDE Fab forming interactions with Arg 99 and Lys 247 and reaching a bound conformation that reproduces the crystal structure orientation as in 4UTA. Cluster 1 includes the structures belonging to the bound state, and the other clusters contain partially bound and unbound structures (Table 2).

3. Discussion

In this study, we have investigated the antigen–EDE Abs binding by using a surrogate model of the protein E antigen that allowed us to perform MD and free energy calculations. This antigen analogue can be produced in experiments, but there are several challenges, as disulfide scrambling and potential oligomerization need to be considered. The antigen derived from protein E is known to bind to broadly neutralizing antibodies, but the molecular determinants and the mechanism of binding is unknown. In this work, we have analyzed in structural details the complexes belonging to EDE1 and EDE2 antibodies. We found common ground in terms of interactions between the antigen and the Abs. In particular, the salt bridge of Lys 247 and the hydrogen bonds of Gly 104 and Arg 99 are conserved in the antigen–Ab association. These residues provide the main enthalpic contribution to the binding, even though the residue partner on the Ab side can differ case by case for the different EDE Ab. The presence of these conserved residues in protein E confirms their functional role in anchoring the Ab to the protein antigen. The MD in the bound state also confirms that Lys 247 and Gly 104 are structurally stable in the association with the Ab, and Arg 99 and Trp 102 are more flexible, fluctuating along the simulations. The relative mobility of these structures provides useful information, which is obtained through the calculation and complements the existing experimental data. Furthermore, Lys 247 can form a salt bridge with Asp 56, but sometimes it is also involved in a hydrogen bond with the oxygen in the side chain of Glu 54. The glycosylation is on the protein E antigen. It does not play a role for the specific EDE1 antibody, but it can affect the interaction in EDE2.[4]

The formation of at least two hydrogen bonds in Gly 104, Arg 99, or Lys 247 represents a critical step for binding to the Ab. Also, the rebound representative structure resembles the original bound conformation (Figure S1), and these particular hydrogen bonds occur (Figures S2 and S3).

Overall, the binding of the antigen to EDE1 C8 Fab corresponded to a reduced mobility of the flexible CDR loops locking these loops in a distinct conformational state,[36] and strong reduction of the mobility of these loops has also been observed in the past in cases of strong antigen–Fab binding.[37]

The antigen has been successfully docked in the binding site of the Fab of EDE1 C8 with a low backbone RMSD value of about 1 Å. This bound structure is stable in long MD runs, providing evidence for a stable binding. The free energy calculations are used to properly estimate the free energy change in the antigen binding process. We found a large change of 5 kcal mol^{-1}, which is in line with antigen binding to the EDE1 C8 Fab. The accurate binding affinity is not known. Differences in the free energy of binding are expected in comparison with the full protein E binding, but protein E is difficult to manage in the MD simulation, owing to its large molecular size. The PMF profile may also change, because of the pathway that is explored in the simulation. Furthermore, we only observed two transitions, which does not ensure that we observed all the possible pathways to binding.

The method produces comparable results to alternative methods that pursue free energy calculations based on a geometrical route.[16,17,35,38,39] Other methods were able to achieve more full transitions from the unbound state to the bound state in previous studies.[40,41] These methods efficiently performed the enhanced sampling, but they were applied to other protein systems different in molecular size from the proteins considered in this study.

In general, the ABF method is a geometrical method, and the bias applied on the potential along the CV can limit the efficiency of the enhanced sampling of the phase space. Alternatively, other methods based on Replica-exchange MD or free energy perturbation (FEP) can lead to more efficient sampling of the phase space. These methods may present challenges requiring large computer power, presenting technical difficulties to perform exchanges for large protein–protein systems. They also require reweighting methods like WHAM, UWHAM, or MBAR to analyze the results. The perturbation of distance restraints[41] is efficient to perform enhanced sampling, but it requires a multistep calculation.

Interestingly, the presence of conserved residues in the antigen, such as Gly 104, Lys 247, and Arg 99, and mutations in the paratope counterpart observed in other EDE antibodies further suggest their key functional role in binding. These residues, being hydrogen bond acceptors or donors, affect antibody binding directly, by participating in the binding interface of the complex. For instance, these residues provide a major enthalpic contribution to the antibody binding. Alternatively, Trp 102 may also play an indirect functional role by contributing to stabilize the overall structure of the complex, as seen in

the microsecond-long simulation. For example, these residues may help rigidifying the CDR loops in the heavy and light chain of EDE1 C8, while also correctly orienting the antigen into the binding site, as pointed out by our MD simulations. Future validation is needed to confirm or disprove such hypotheses about the mechanism. In this respect, future site-directed mutagenesis and protein engineering on these hotspot residues may have prospective applicability in designing novel antigens with enhanced binding affinity for broadly neutralizing antibodies directed to the DENV. Furthermore, the design of small peptide antigens that bind to EDE1 antibodies may lead to the identification of novel immunogens. Reproducing the structural conformation at the binding interface of the hydrogen bond network formed by the hotspot residues may pave the way for a de novo protein design of molecules capable of triggering an effective immune response against DENV. Similar approaches have been key in the fight against another viruses like influenza.[42] Computationally, the same method used here can be used to screen novel designs in synergy with experimental thermodynamic measurements. Finally, our structural and thermodynamic observations may stimulate further work to clarify possible structural implications of Gly 104 and Lys 247 in the antigen binding to EDE Abs. These key hotspot interactions can also be used to develop novel Abs as therapeutic agents, retaining the interaction with these hotspots by using residues capable of forming contacts, but making mutations in other regions that are not critical for the potency.

4. Conclusions

Combining structural alignments with MD simulations in the EDE1 Abs, we identified the critical elements that provide a major energetic contribution to the association of antigens from protein E with Abs. Possible molecular insights into the binding mechanism have been explored by using a surrogate molecular entity resembling protein E, which forms native salt bridges and hydrogen bonds, including inferences on the light of high-resolution crystal structures of dengue Fab complexes. The molecular determinants, free energy profile, and binding mechanism provide inspiration for potential strategies in protein engineering to design novel immunogens of protein E against DENV.

Conflict of Interest

The authors declare no conflict of interest.

Keywords: antibodies · dengue virus · free energy · molecular modeling · potential of mean force

[1] Y.-S. Tian, Y. Zhou, T. Takagi, M. Kameoka, N. Kawashita, *Chem. Pharm. Bull.* **2018**, *66*, 191 – 206.
[2] D. Kuroda, H. Shirai, M. P. Jacobson, H. Nakamura, *Protein Eng. Des. Sel.* **2012**, *25*, 507 – 522.
[3] G. Fibriansah, K. D. Ibarra, T.-S. Ng, S. A. Smith, J. L. Tan, X.-N. Lim, J. S. G. Ooi, V. A. Kostyuchenko, J. Wang, A. M. de Silva, E. Harris, J. E. Crowe, S.-M. Lok, *Science* **2015**, *349*, 88 – 91.
[4] A. Rouvinski, P. Guardado-Calvo, G. Barba-Spaeth, S. Duquerroy, M.-C. Vaney, C. M. Kikuti, M. E. Navarro Sanchez, W. Dejnirattisai, W. Wongwiwat, A. Haouz, C. Girard-Blanc, S. Petres, W. E. Shepard, P. Despres, F. Arenzana-Seisdedos, P. Dussart, J. Mongkolsapaya, G. R. Screaton, F. A. Rey, *Nature* **2015**, *520*, 109 – 113.
[5] P. W. Rose, B. Beran, C. Bi, W. F. Bluhm, D. Dimitropoulos, D. S. Goodsell, A. Prilc, M. Quesada, G. B. Quinn, J. D. Westbrook, J. Young, B. Yukich, C. Zardecki, H. M. Berman, P. E. Bourne, *Nucleic Acids Res.* **2011**, *39*, D392 – D401.
[6] A. Fiser, A. Sali, *Methods Enzymol.* **2003**, *374*, 461 – 491.
[7] B. Webb, A. Sali, *Curr. Protoc. Bioinform.* **2016**, *54*, 5.6.1 – 5.6.37.
[8] J. C. Phillips, R. Braun, W. Wang, J. Gumbart, E. Tajkhorshid, E. Villa, C. Chipot, R. D. Skeel, L. Kale, K. Schulten, *J. Comput. Chem.* **2005**, *26*, 1781 – 1802.
[9] R. B. Best, X. Zhu, J. Shim, P. E. M. Lopes, J. Mittal, M. Feig, A. D. Mackerell, *J. Chem. Theory Comput.* **2012**, *8*, 3257 – 3273.
[10] W. L. Jorgensen, J. Chandrasekhar, J. D. Madura, *J. Chem. Phys.* **1983**, *79*, 926 – 935.
[11] T. Darden, D. York, L. Pedersen, *J. Chem. Phys.* **1993**, *98*, 10089 – 10092.
[12] J. P. Ryckaert, G. Ciccotti, H. J. C. Berendsen, *J. Comput. Phys.* **1977**, 327 – 341.
[13] R. Chen, L. Li, Z. Weng, *Proteins Struct. Funct. Bioinf.* **2003**, *52*, 80 – 87.
[14] K. Wiehe, B. Pierce, J. Mintseris, W. W. Tong, R. Anderson, R. Chen, Z. Weng, *Proteins Struct. Funct. Bioinf.* **2005**, *60*, 207 – 213.
[15] B. G. Pierce, Y. Hourai, Z. Weng, *PLOS ONE* **2011**, *6*, 1 – 6.
[16] E. Darve, A. Pohorille, *J. Chem. Phys.* **2001**, *115*, 9169 – 9183.
[17] E. Darve, D. Rodríguez-Gómez, A. Pohorille, *J. Chem. Phys.* **2008**, *128*, 144120.
[18] M. Lapelosa, *J. Chem. Theory Comput.* **2017**, *13*, 4514 – 4523.
[19] E. F. Pettersen, T. D. Goddard, C. C. Huang, G. S. Couch, D. M. Greenblatt, E. C. Meng, T. E. Ferrin, *J. Comput. Chem.* **2004**, *25*, 1605 – 1612.
[20] W. Humprey, A. Dalke, K. Schulten, *J. Molec. Graphics* **1996**, *14*, 33 – 38.
[21] L. A. Kelley, S. P. Gardner, *M. J. Sutcliffe. Protein Eng.* **1996**, *9*, 1063 – 1065.
[22] T. W. Allen, O. S. Andersen, B. Roux, *Biophys. Chem.* **2006**, *124*, 251 – 267.
[23] I.-C. Lin, M. E. Tuckerman, *J. Phys. Chem. B* **2010**, *114*, 15935 – 15940.
[24] J. D. Chodera, D. L. Mobley, M. R. Shirts, R. W. Dixon, K. Branson, V. S. Pande, *Curr. Opin. Struct. Biol.* **2011**, *21*, 150 – 160.
[25] M. Lapelosa, E. Gallicchio, R. M. Levy, *J. Chem. Theory Comput.* **2012**, *8*, 47 – 60.
[26] E. Gallicchio, R. M. Levy, *Adv. Prot. Chem. Struct. Biol.* **2011**, *85*, 27 – 80.
[27] M. Lapelosa, C. F. Abrams, *J. Chem. Theory Comput.* **2013**, *9*, 1265 – 1271.
[28] K. Wang, J. D. Chodera, Y. Yang, M. R. Shirts, *J. Comput.-Aided Mol. Des.* **2013**, *27*, 989 – 1007.
[29] B. Lai, G. Nagy, J. A. Garate, C. Oostenbrink, *J. Chem. Inf. Model.* **2014**, *54*, 151 – 158.
[30] D. J. Cole, J. Tirado-Rives, W. L. Jorgensen, *J. Chem. Theory Comput.* **2014**, *10*, 565 – 571.
[31] Y. Miao, V. A. Feher, J. A. McCammon, *J. Chem. Theory Comput.* **2015**, *11*, 3584 – 3595.
[32] J. A. Morrone, A. Perez, J. MacCallum, K. A. Dill, *J. Chem. Theory Comput.* **2017**, *13*, 870 – 876.
[33] D. Kilburg, E. Gallicchio, *Front. Mol. Biosci.* **2018**, *5*, 22.
[34] G. Lamothe, T. E. Malliavin, *BMC Struct. Biol.* **2018**, *18*, 4.
[35] M. Lapelosa, *Biophys. Chem.* **2018**, *232*, 22 – 28.
[36] E. M. Herold, C. John, B. Weber, S. Kremser, J. Eras, C. Berner, S. Deubler, M. Zacharias, J. Buchner, *Sci. Rep.* **2017**, *7*, 12276.
[37] E. Rujas, N. Gulzar, K. Morante, K. Tsumoto, J. K. Scott, J. L. Nieva, J. M. Caaveiro, *J. Virol.* **2015**, *89*, 11975 – 11989.
[38] D. Rodríguez-Gómez, E. Darve, A. Pohorille, *J. Chem. Phys.* **2004**, *120*, 3563 – 3578.
[39] J. Hénin, A. Pohorille, C. Chipot, *J. Am. Chem. Soc.* **2005**, *127*, 8478 – 8484.
[40] J. C. Gumbart, B. Roux, C. Chipot, *J. Chem. Theory Comput.* **2013**, *9*, 3789 – 3798.
[41] J. W. Perthold, C. Oostenbrink, *J. Chem. Theory Comput.* **2017**, *13*, 5697 – 5708.
[42] K. Das, L. C. Ma, R. Xiao, B. Radvansky, J. Aramini, L. Zhao, J. Marklund, R. L. Kuo, K. Y. Twu, E. Arnold, R. M. Krug, G. T. Montelione, *Proc. Natl. Acad. Sci. USA* **2009**, *105*, 13093 – 13098.

Received: June 27, 2018

